B1-Field Inhomogeneity Problem of MRI: Basic Investigations on a Head-Tissue-Simulating Cylinder Phantom Excited by a Birdcage-Mode

A. Rennings[1], L. Chen[1], S. Otto[2], and D. Erni[1]
[1]General and Theoretical Electrical Engineering (ATE) and [2]High-Frequency Engineering (HFT),
Faculty of Engineering, University of Duisburg-Essen, 47048 Duisburg, Germany
andre.rennings@uni-duisburg-essen.de

Abstract— **The RF-field inhomogeneity problem of MRI at high resonance frequency is investigated from an electromagnetic viewpoint by numerical FEM simulations. The evaluation is based on a simple two-dimensional model including a cylinder phantom with spatially constant but frequency-dependent material parameters of a head-tissue-simulating liquid (HTSL) and an imposed field-exciting surface current distribution between the phantom's surface and a surrounding perfect electric conductor (PEC) shield. This simple arrangement has been chosen intentionally in order to reduce the set of parameters to a minimum, allowing clear statements about the applicability of the widely used first-order circularly polarized (CP) excitation mode. The coefficient of variation (CoV) of the |B1+| distribution is a suitable figure of merit for the specification of the homogeneity. Only two parameters of the arrangement have been varied – the excitation frequency ranging from 30 MHz up to 450 MHz and the diameter of the phantom ranging from a few centimeters up to 25 cm, which covers more or less every MR head imaging scenario. Two characteristic |B1+| distributions will be introduced, which separate the frequency/diameter combinations into three different regions, a first one with a quasi homogeneous pattern, a second one where an interference pattern — the central brightening — occurs, and a last one, where only a quite weak center amplitude smaller then the mean value is excited.**

Keywords- Electromagnetic-biological interactions, magnetic resonance imaging (MRI), RF coils, birdcage mode, numerical EM field simulation

I. INTRODUCTION

In magnetic resonance imaging (MRI) the birdcage resonantor is probably the most popular RF coil concept, due to its simple and robust operation [1]. At the first-order resonance a sampled full-wave-length current distribution with a phase shift of 360° is established. By applying a quadrature feed a "propagating" wave in azimuthal direction is obtained and a nearly perfect spatially constant B1+ magnitude is excited, which is the so-called circularly-polarized component [1]. But this is only true for the unloaded, i.e., air-filled birdcage resonator. In practice the RF coil is loaded with a part of the human body, having a frequency-dependent permittivity and conductivity. For high- ($B_0 \geq 3$ Tesla) and especially for ultra-high field ($B_0 \geq 7$ Tesla) MRI systems the |B1+| distribution deviates from the desired spatially constant field pattern [1].

Here, we systematically investigate this issue for the case of a head-tissue-simulating cylinder phantom. Only the diameter of the cylinder phantom and the MR frequency, which is proportional to the B_0, are varied. Typical patterns for the |B1+| and the local specific absorption rate (SAR) are discussed and a range for the applicability of the first-order birdcage-mode is proposed.

II. MATERIALS AND METHODS

The electromagnetic field problem was solved numerically by the full-wave finite element method (FEM) solver COMSOL Multiphysics. The RF field pattern quality is evaluated via its mean-value and the coefficient of variation (short CoV, which normalizes the standard deviation to the mentioned mean-value), of the |B1+| distributions. Additional to the magnetic-field-based figures of merit (FoM), the maximal local specific absorption rate (SAR), which depends on the electric field, is considered here. The SAR peak and the |B1+| mean value are normalized to the accepted power and its square root, respectively. This is not necessary for the CoV, which is already normalized by definition. All scalar values are evaluated only inside the phantom, which mimics the body part to be imaged. In [2], such an investigation — there only based on the CoV(|B1+|) — is presented for cylindrical phantoms filled with body tissue simulating liquid (BTSL) [3]. Here, we focus on the head imaging scenario as already mentioned in the introduction. Due to the broad-band investigation starting at a frequency of 30 MHz ranging up to 450 MHz the material properties of the phantom filled with head-tissue-simulating liquid (HTSL) [3] must be adjusted correspondingly to the MR frequency. The frequency dependent material parameters for the standardized HTSL are given in Fig. 1. The raw data from [3] has been smoothed by a piecewise cubic Hermite interpolation.

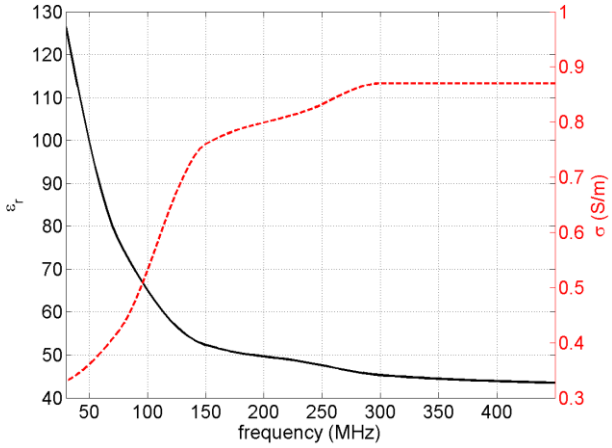

Figure 1. Relative permittivity and conductivity for the standardized head-tissue-simulating liquid (HTSL) as a function of frequency. The raw data from [3] has been smoothed by a piecewise cubic Hermite interpolation.

III. Ideal 2-D Setup Including Head Phantom, Impressed Current Sheet and PEC Shield

For the idealized setup depicted in Fig. 2 only the phantom diameter and the RF excitation frequency were varied. Due to the two-dimensionality of the problem, one simulation took less than 10 seconds, allowing to reduce the step width to 10 mm and 5 MHz, respectively, yielding reasonably smooth two-dimensional contour plots for the CoV of the |B1+| pattern, as given in Fig. 3. The mean-value and standard-deviation of the field pattern were calculated inside the whole head phantom via the built-in MATLAB routines. For each frequency-domain FEM simulation, the phantom's material parameters were updated as specified in the corresponding standard [3].

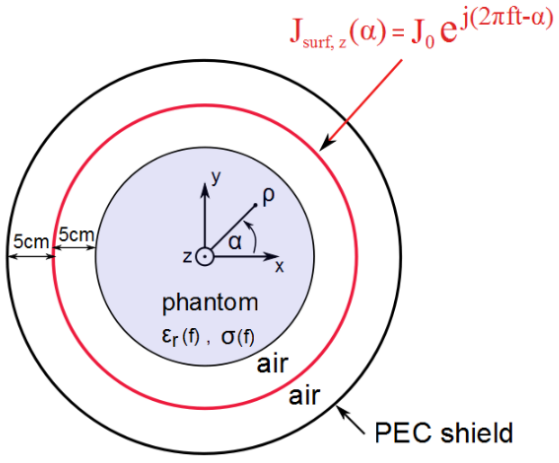

Figure 2. Ideal 2-D model including a cylinder phantom with frequency-dependent material parameters and varying diameter, the active sheet (in red) with imposed surface current (J_0 = 1 A/m) distribution 5 cm away from the phantom's surface, and the PEC shield with a further 5 cm separation.

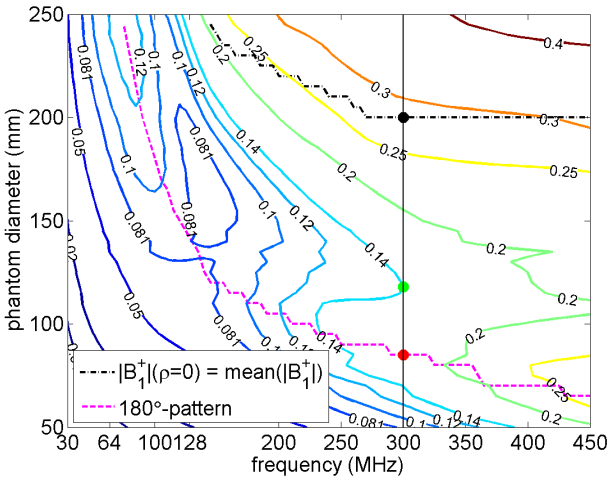

Figure 3. Contour plot for the CoV of the |B1+| pattern inside the head phantom as a function of frequency (x-axis) and phantom diameter (y-axis) – with border lines, where typical field pattern occur (cf. Fig. 4).

The contour plot for the CoV can be divided into three different regions. In Fig. 3 border lines have been introduced to divide the whole diameter-frequency field into these regimes. Along the two border lines the |B1+| distribution shows a very characteristic pattern. For MR frequencies above 128 MHz the CoV is going through a local minimum for varied diameters. Thus we have a third characteristic pattern – the one with a minimal CoV (for varied diameter). This can be interpreted as a locally optimal operation point, which is always located between the two border lines.

Due to the symmetry of the EM field problem, as shown in Fig. 2, the pattern are rotationally symmetric and therefore depend only on the radius coordinate ρ. Thus 1-D plots are sufficient. Here characteristic pattern will be investigated for a MR frequency of 300 MHz, which corresponds to a B_0 of 7 Tesla -- a magnetic flux density, where the applicability of the birdcage mode is disputable.

In Fig. 4 the three characteristic |B1+| patterns together with the corresponding mean-values are depicted. The three distributions have two characteristic features in common: First, a constructive interference at the center (ρ = 0), and second, a destructive interference at around ρ = 45 mm. The characteristic feature of the first pattern (red curve in Fig. 4) is its destructive interference with a local amplitude minimum at the phantom's surface – thus we denote it as the "180°-pattern". In addition to the minimal CoV, the second pattern (green curve in Fig. 4) seems to have a special shape as well, with a surface value that is equal to the mean. Finally, the special feature of the third depicted pattern (black curve in Fig. 4) would be the "center-equals-mean" type, which is self explaining.

The typical distributions along the border-lines might be defined as the beginning and end of the central-brightening phenomenon for head imaging, respectively.

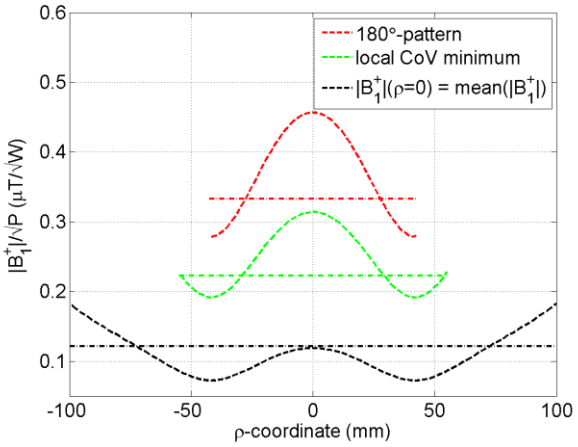

Figure 4. |B1+| distributions and corresponding mean value levels at 300 MHz, representing characteristic patterns: First, the "180°-pattern" with local field minimum at the phantom's surface (top); second, the "surface-equals mean" distribution (middle), which yields a local CoV minimum; and third, the "center-equals-mean" pattern (bottom).

Below the magenta border line of Fig. 3 a quite constant |B1+| excitation with no local field minima inside the phantom is ensured (this minimum is located at the phantom's surface), whereas above the black border line, a quite weak center amplitude, smaller then the mean value is predicted by our 2-D model.

Similarly to the CoV, the maximal SAR value detected inside the phantom for all the diameter/frequency combinations is given in the 2-D contour plot of Fig. 5.

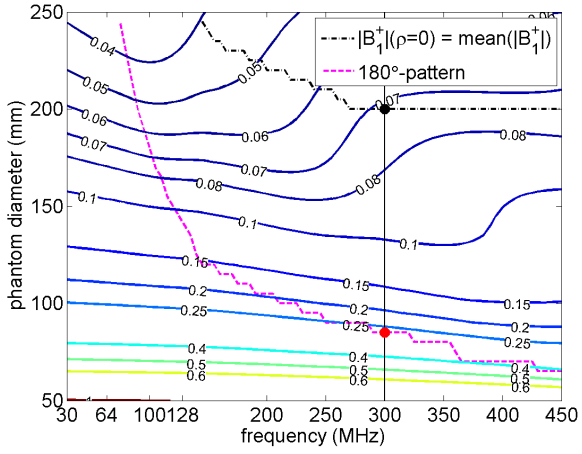

Figure 5. Contour plot of the peak SAR value inside the head phantom as a function of frequency (x-axis) and phantom diameter (y-axis) – with the same border lines as in Fig. 3. The corresponding , where typical SAR field distributions occur (cf. Fig. 6).

The two border lines, which were defined on the bases of specific |B1+| pattern, are plotted here as well. The behavior of the peak SAR will be discussed next. Below the "180°-pattern" border-line the value remains approximately constant with increased frequency. In between the two border-lines the SAR_{max} is increased quite strongly at a certain diameter-dependant frequency (cf. Fig. 5). Above the "center-equals-mean" border the value seems to be again rather constant with increasing frequency. Hence, the peak SAR value depends strongly on frequency only between the two border-lines, a diameter-frequency-range, where the central-brightening phenomenon occurs.

Next the SAR distribution is investigated at the two |B1+| based border-lines (cf. Fig. 5) -- again for the 300-MHz-case. As depicted in Fig. 6, at the center of the phantom all SAR distributions vanish due to the harmonic current excitation.

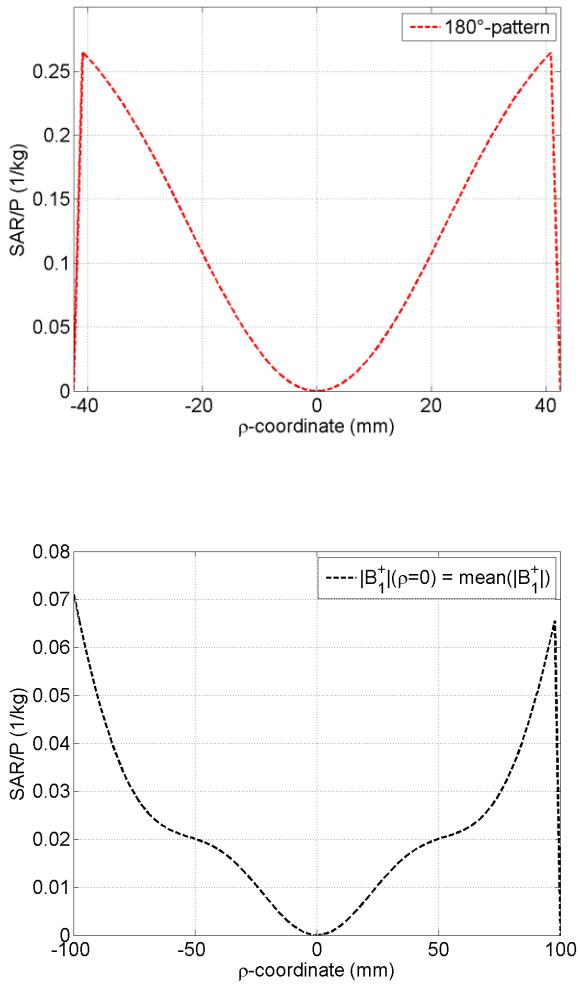

Figure 6. Local SAR distributions normalized to the overall absorpted power at the two border lines for 300 MHz (cf. Fig. 5): the "180°-B1-pattern" corresponds to a parabolic SAR shape (top, electric field magnitude roughly increases linearly with radius) and the "center-equals-mean-B1-pattern" corresponds to a "bull-like" SAR shape with two inflexion points (bottom).

The "180°-B1-pattern" corresponds to a parabolic SAR shape. The corresponding electric field magnitude roughly increases linearly with radius. For the "center-equals-mean-B1-pattern" we observe a more complicated SAR shape with two inflexion points at $\rho = 45$ mm, a location where also the |B1+| minimum is located (cf. Fig. 4).

IV. Conclusion and Outlook

The RF-field inhomogeneity problem of head MRI at high resonance frequency has been investigated from an electromagnetic viewpoint by numerical FEM simulations. Several characteristic |B1+| and SAR distributions have been introduced, which separate the frequency/diameter combinations into different regimes. Based on these investigations the diameter/frequency combinations that can be handled by the simple birdcage resonantor are predicted.

In future investigations we will consider also 3-D body models in order to evaluate the influence of the shape of the body part to be imaged. Additionally, inhomogeneous tissue distributions will be used.

References

[1] J. Jin, Electromagnetic Analysis and Design in Magnetic Resonance Imaging. CRC Press Inc, 1998.

[2] A. Rennings, L. Chen, F. Wetterling, M.E. Ladd, and D. Erni, "Electromagnetic field evaluations inside a body-tissue-simulating cylinder phantom excited by an ideal first-order circularly polarized mode", ISMRM'12 in Melbourne, Australia, paper 5985.

[3] A. Christ, T. Samaras, A. Klingenböck, N. Kuster, "Characterization of the electromagnetic near-field absorption in layered biological tissue in the frequency range from 30 MHz to 6000 MHz," Phys Med Biol. 2006;51:4951-65.